Optical study of $0.65PbMg_{1/3}Nb_{2/3}O_3$-$0.35PbTiO_3$ thin films

K. Y. Chan, W. S. Tsang, C. L. Mak and K. H. Wong

Department of Applied Physics, The Hong Kong Polytechnic University, Hung Hom, Hong Kong, China

ABSTRACT

$0.65PbMg_{1/3}Nb_{2/3}O_3$-$0.35PbTiO_3$ (PMN-PT) thin films with different deposition temperatures have been fabricated on (001)MgO single crystal substrates using pulsed laser deposition (PLD). X-ray diffraction (XRD) shown that the films are epitaxially grown on (001)MgO substrate. Spectroscopic ellipsometer (SE) was used to characterize the optical properties including refractive index as well as extinction coefficient of these PMN-PT films in the range of 0.75 – 3.5 eV. By fitting the measured ellipsometeric spectra, film thicknesses, surface roughness and optical properties were derived for all PMN-PT films. The film thickness and surface roughness obtained by SE were consistent with these measured by scanning electron microscopy (SEM) and atomic force microscopy (AFM) respectively. The optical band gap energies of PMN-PT films were deduced from the obtained extinction coefficients using Tauc equation. These values were comparable to those obtained by optical transmittance measurements. Our analysis revealed that the optimum refractive index emerges as the film fabricated at ~670^{o}C.

I. INTRODUCTION

The good electro-optic properties of ferroelectrics coupled with the advances made recently in thin film fabrication technology allow thin-film ferroelectrics to be considered as a formidable candidate for many integrated optic devices. Potential applications include low-voltage electro-optic switches, compact low-threshold gain devices and second-harmonic generators.[1] Among various ferroelectrics for optical applications, $0.65PbMg_{1/3}Nb_{2/3}O_3$-$0.35PbTiO_3$ (PMN-PT) is one of the most promising ferroelectric candidates due to its extremely high electro-optic coefficient and strong photorefractive effect.[2] Indeed, PMN-PT has an electro-optic coefficient larger than the best value reported for $(Pb,La)(Zr,Ti)O_3$ thin films.[3]

In this paper, we report the changes of refractive indices and extinction coefficients of PMN-PT films as a function of fabrication temperature. PMN-PT films were grown on MgO single crystal using PLD method. The choice of using MgO substrate is based on the small lattice mismatch and large difference in refractive index between PMN-PT film and MgO substrate. MgO single crystal has a lattice constant of 4.21 Å which is close to that of PMN-PT (4.02 Å).[4, 5] The refractive index of 0.7PMN-0.3PT ceramic is 2.598 at 633 nm,[2] and this value is much larger than that of MgO (1.734) at 650 nm.[6] A larger refractive index difference between the film and substrate increases the amplitude of oscillations of ellipsometric spectra, and thus enhances the accuracy of ellipsometric measurements. After obtaining the extinction coefficients of PMN-PT films, the absorption coefficients, and hence the band gap energies of these films were estimated. Such band gap values were compared to those values measured by optical transmittance measurements. Good agreement was found between the two sets of data. Finally, the effects of deposition temperature on the optical properties as well as the band gap energies of PMN-PT films were discussed.

II. EXPERIMENT

PMN-PT films were grown on (001)MgO single crystal substrates by PLD using an ArF excimer-laser. Three different deposition temperatures 630^{o}C, 670^{o}C and 710^{o}C were employed in our experiment. All the 25-mm diameter and 5-mm thick cylindrical PMN-PT targets were homemade from single phase powders pressed at 80 MPa and sintered at 900^{o}C for 10 hours. Unless stated otherwise, the following conditions for the deposition of PMN-PT films were employed in all cases. The PMN-PT films were deposited in a high vacuum chamber equipped with a rotating holder. The distance between the substrate and the target was kept at 5 cm throughout the experiment. The conditions of 6 Hz laser repetition rate and 4 J/cm^2 energy density were used. The ambient oxygen pressure was 200 mTorr and the deposition time was 20 minutes. After deposition, the as-grown PMN-PT films were post-annealed at the deposition temperature and pressure for another 10 minutes. Afterwards, the films were cooled naturally to room temperature. X-ray diffraction (XRD, Philip PW3710) using Cu K_{α} radiation, scanning electron microscopy (SEM, Leico, Stereoscan440) and atomic force microscopy (AFM) were employed to characterize the structural properties of our PMN-PT films. For optical analyses, spectroellipsometry (SE) measurements were carried out by a spectroscopic phase modulated ellipsometer (Jobin Yvon UVISEL) at photon energy between 0.75 eV to 3.5 eV with 0.01 eV interval. An incidence angle of 70^{o} was used throughout our measurements. Finally, optical transmittance measurement was carried out by a two-beam spectrophotometer (Shimadzu UV-2101).

III. RESULTS AND DISCUSSION

The XRD $\theta - 2\theta$ profiles of the PMN-PT/MgO films with different deposition temperatures are shown in Fig. 1. Highly oriented PMN-PT films of perovskite phase are observed. The out-of-plane lattice constants calculated from the diffraction angles of (002) peak of PMN-PT films with deposition temperature of 630^{o}C, 670^{o}C and 710^{o}C were 3.99 Å, 4.02 Å and 4.02Å, respectively. The full-width-half-maximum (FWHM) of the rocking curves for all PMN-PT films were 1.65^{o}, 0.79^{o} and 2.3^{o}. To give an idea of the instrumentation limit of our XRD machine, the FWHM value for MgO substrate of is ≤ 0.2°. XRD ϕ-scans of the (202)PMN-PT and (202)MgO were performed to confirm the epitaxy of our films. Inset of Fig. 1 shows a typical ϕ-scan for PMN-PT film deposited at 670^{o}C. The peaks of PMN-PT and MgO are at the same position and separated by 90^{o}. This clearly shows the four-folded symmetry of both the film and the substrate. Our XRD results indicate that all PMN-PT films are cube-on-cube grown on (001)MgO substrates with an in-plane epitaxial relationship of (001)PMN-PT||(001)MgO.

The surface and cross-section SEM images of PMN-PT films deposited at 630^{o}C, 670^{o}C and 710^{o}C were measured. In general, the surfaces are smooth and crack-free for films deposited at 630^{o}C and 670^{o}C, while the sample surface is slightly rougher for film deposited at 710^{o}C. According to our cross-section SEM images, the film and the substrate are easily distinguished for all samples. Figure 2 manifests the SEM images of PMN-PT film deposited at 670^{o}C. Here, thickness of the film is and the root mean square (rms) roughness were found to be ~ 655 nm and ~ 3.8 nm, respectively. These are very close to those obtained by SE. Indeed, all films have similar features with a rms roughness less than 10 nm (Table I).

Figure 3 shows the ellipsometric spectra of experimental and simulated ellipsometric parameters, I_S and I_C, for PMN-PT film deposited at 710°C. Generally, SE measures the traditional ellipsometric angles, ψ and Δ, as functions of photon energy in the experiment. In this study, however, spectroscopic phase modulated method was used. In this method, the measuring parameters are I_S and I_C instead of ψ and Δ. The Details of this transformation can be found in elsewhere.[7,8] The optical properties of oxygen-octahedral ferroelectrics are dominated by the BO_6 octahedra, which governs the low lying conduction bands and the highest valence bands. This lowest energy oscillator is the largest contributor to the dispersion of the refractive index. Other ions in the structure contribute to the higher-lying conduction band and have a small effect on the optical properties of these ferroelectrics. Hence, a Lorentz oscillator model of the dielectric function with four oscillators,

$$\varepsilon(\omega) = \varepsilon_{\infty} + \sum_{j=1}^{4} \frac{f_j \omega_{oj}^2}{\omega_{oj}^2 - \omega^2 + i\gamma_j \omega} \qquad \textbf{(1)}$$

has been used to describe this dominated interband oscillator of PMN-PT. The parameters ε_{∞}, f_j, ω_o and γ_j are the contributions of high energy excitations, oscillator weightings, resonance energies and half widths respectively. Our initial analysis was based on a single-layer Lorentz model. In our fitting, the refractive index of our substrate is obtained from MgO single crystal.[6] Poor agreement, however, was obtained with the experimental data. In subsequent analysis, we modified the single-layer Lorentz model into a double-layer Lorentz model (inset of Fig. 3). In this model, we assume that the films consist of two layers – a bottom bulk PMN-PT layer and a surface layer that composed of bulk PMN-PT as well as voids. These voids in the surface layer

were mainly caused by surface roughness. Here, f_{v2} refers to the volume percentage of air in the surface layer. The net optical constants of the mixed layer (PMN-PT + void) were calculated using Bruggeman effective medium approximation. Depending on the double-layer Lorentz model, we analyzed the data over the spectra range 0.75 – 3.5 eV, good fits between the simulated values of I_S as well as I_C and the experimental data were obtained. The solid lines in Fig. 3 denote these fitted results. Table I lists the layer thicknesses of the bulk material and surface layer for different PMN-PT films obtained from our modified Lorentz model, SEM and AFM measurements.

Figure 4 shows the refractive index dispersion curves of PMN-PT films deposited at different temperatures based on eqt. (1). In general, the refractive index n appears to be continuously increased nonlinearly over the whole energy range from 0.75 to 3.5 eV. Indeed, it increases more sensitively at higher energies. However, the extinction coefficient k is fairly flat below 2.5 eV. This behavior is typical of an insulator or semiconductor in the range of energy near the band gap. Below the band gap, transmission dominates with a tiny extinction coefficient. As the band gap energy is approached from below, both n and k increase with k approaches a resonance characterized by one of the oscillators in the Lorentz model. Meanwhile the refractive index of PMN-PT film increases from deposition temperature of 630^{o}C to 670^{o}C, but it decreases again at 710^{o}C. This lowering of refractive index at higher temperature may be caused by the loss of PbO. It is well known that PbO would evaporate and escape from the film surface at an elevated post-deposition annealing temperature. In this circumstance, PbO evaporation and grain densification increase the film's porosity and hence locally reduce the density of film. This phenomenon has been reported in lead-based ferroelectric films.[9] This reduction of film's density would certainly decrease the refractive index of the film. As a result,

the refractive index of film decreases with higher post-deposition annealing temperature. Figure 5 shows the extinction coefficient dispersion curves of PMN-PT films. According to Fig. 5, the extinction coefficient of PMN-PT film deposited at 710^{o}C is larger, particularly in higher energy region than those of other two films. This larger extinction coefficient may be due to a larger grain size, resulting in a stronger scattering of light.

As we have mentioned, the optical properties of PMN-PT are dominated by inter-band electronic transitions between the lower lying conduction bands and the upper valence bands of BO_6 octahedra. It is of great interest to investigate the change of the optical band gap of PMN-PT films deposited at different temperatures. The absorption coefficients of the films can be obtained from extinction coefficients using:

$$\alpha = \frac{4\pi}{\lambda} k \qquad \textbf{(2)}$$

where k is the extinction coefficient, α is the absorption coefficient and λ is the wavelength. Then, the optical band gap energies of PMN-PT films were deduced from the absorption coefficient α and the energy of the incident light $h\nu$ using Tauc equation:[10]

$$(\alpha h\nu)^2 = B(h\nu - E_g) \qquad \textbf{(3)}$$

where B is a constant and E_g is the band gap energy. Inset of Fig. 5 shows the dependence of the absorption coefficients $(\alpha h\nu)^2$ on the photon energy for PMN-PT films deposited at 710^{o}C. By extrapolating the linear portion curve of the curve to zero, the band gap energies obtained for all PMN-PT films deposited at different temperatures are close to ~ 3.50 eV.

In order to verify the values of the band gap energies of PMN-PT films, optical transmittance measurements were carried out. Figure 6 shows the transmittance spectra of PMN-PT films. The transmittance curve of PMN-PT film with 710^{o}C deposition temperature shows a larger absorption at wavelengths below band gap, which is agreed with the extinction coefficient

obtained by SE measurements. Figure 7 shows the dependence of the absorption coefficients $(\alpha h\nu)^2$ on the photon energy obtained from the transmittance spectra. Similarly there is no observable change in the band gap energies as we changed the deposition temperature from 630°C to 710°C. We notice that the two sets of values of the band gaps obtained by two different techniques take on similar trend and values. They both indicate that band gap energy of PMN-PT film is not sensitive to deposition temperature. As compared with the change in composition[11] where the band gap energy changes by ~3 % as we changed the composition (1-x)PMN-xPT ($0<x<0.4$).

IV. CONCLUSION

$0.65PbMg_{1/3}Nb_{2/3}O_3$-$0.35PbTiO_3$ (PMN-PT) thin films with different deposition temperatures have been successfully fabricated on (001)MgO single crystal substrates by pulsed laser deposition. SE was used to characterize the depth-profile, refractive index and extinction coefficient of these films. It is found that the refractive index of PMN-PT film decreases at higher deposition temperature, while its extinction coefficient is larger than those of the other two films. The surface roughness and the film thickness of the films obtained from double-layer Lorentz model are consistent with those measured by SEM and AFM. The transmittance results show that the change in the optical band gap energy of PMN-PT film with deposition temperature is less sensitive than that with composition.

FIGURE CAPTIONS

Figure 1 X-ray diffraction patterns of PMN-PT films deposited at (a) 630°C, (b) 670°C and (c) 710°C grown on MgO substrates. Inset shows the XRD ϕ scans of the (a) PMN-PT(202) and (b) MgO(202) with deposition temperature 670°C.

Figure 2 SEM micrographs show the (a) surface morphology and (b) cross-section of PMN-PT film deposited at 670°C.

Figure 3 Spectra of the ellipsometric parameters I_S and I_C as functions of photon energy from PMN-PT films deposited 670°C. The (+) and (o) are the measured I_S and I_C values, respectively, while the solid lines are model fitting. Inset shows the schematic picture of the double-layer Lorentz model.

Figure 4 Refractive indices of PMN-PT films deposited at 630°C (●), 670°C (■) and 710°C (▲).

Figure 5 Extinction coefficients of PMN-PT films deposited at 630°C (●), 670°C (■) and 710°C (▲). Inset shows the dependence of $(\alpha h\nu)^2$ obtained from the fitted extinction coefficients against the photon energy for PMN-PT film deposited at 710°C.

Figure 6 Transmission spectra of PMN-PT films on MgO substrates with different deposition temperatures.

Figure 7 The dependence of $(\alpha h\nu)^2$ versus $h\nu$ obtained from the transmission spectra of PMN-PT films on MgO substrates with different deposition temperatures.

References

1. Y. Xu, *Ferroelectric Materials and Their Applications* (North-Holland, Amsterdam, 1991).
2. Y. H. Lu, J. J. Zheng, M. C. Golomb, F. L. Wang, H. Jiang, and J. Zhao, *Appl. Phys. Lett.* **74**, 3764 (1999).
3. H. Adachi, T. Mitsuyu, O. Yamazaki, and K. Wasa, *J. Appl. Phys.* **60**, 736 (1986).
4. V. Nagarajan, C. S. Ganpule, B. Nargaraj, S. Aggarwal, S. P. Alpay, and A. L. Roythurd, *Appl. Phys. Lett.* **75**, 4183 (2000).
5. M. Tynina, J. Levoska, A. Sternberg, and S. Leppävuori, *J. Appl. Phys.* **86**, 5179 (1999).
6. R. E. Stephens and I. H. Maalitson, *J. Res. Natl. Bur. Stand.* **49**, 249 (1952).
7. C. L. Mak, B. Lai, K. H. Wong, C. L. Choy, D. Mo and Y. L. Zhang, *J. Appl. Phys.* **89**, 4491 (2001).
8. K. M. Yeung, W. S. Tsang, C. L. Mak and K. H. Wong, *J. Appl. Phys.* **92**, 3636 (2002).
9. Fox, G. R. and Krupanidhi, S. B., *Mater J. Res.*, **7**, 3039 (1992).
10. J. C. Tauc, *Optical Properties of Solids* (North-Holland, Amsterdam, 1972), p.372.
11. K. Y. Chan, W. S. Tsang, C. L. Mak and K. H. Wong, *Phys. Review B,* **69**,144111 (2004).

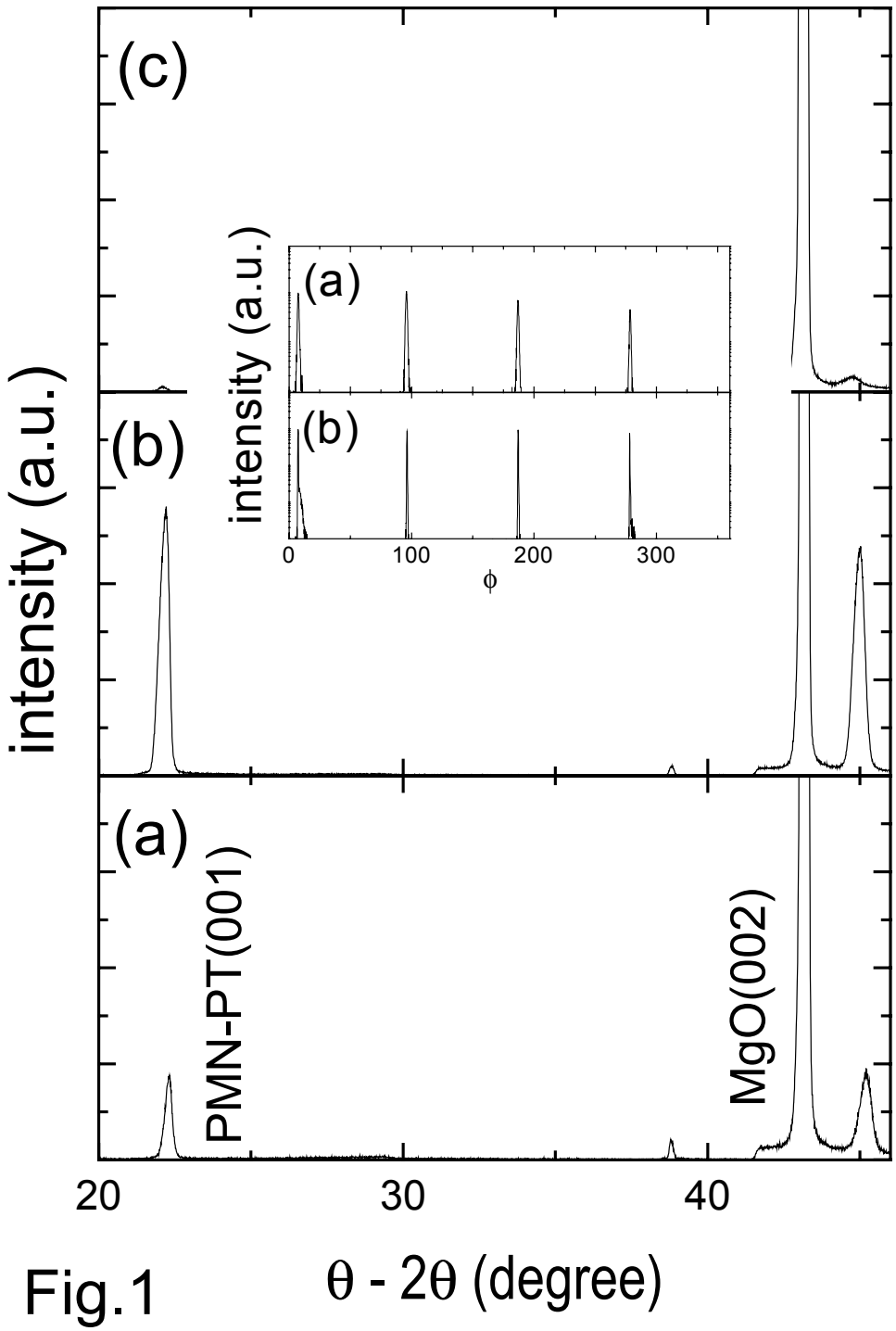
(c)
(b)
(a)
intensity (a.u.)
intensity (a.u.)
(a)
(b)
0
100
200
300
ϕ
PMN-PT(001)
MgO(002)
20
30
40
θ - 2θ (degree)

Fig.1

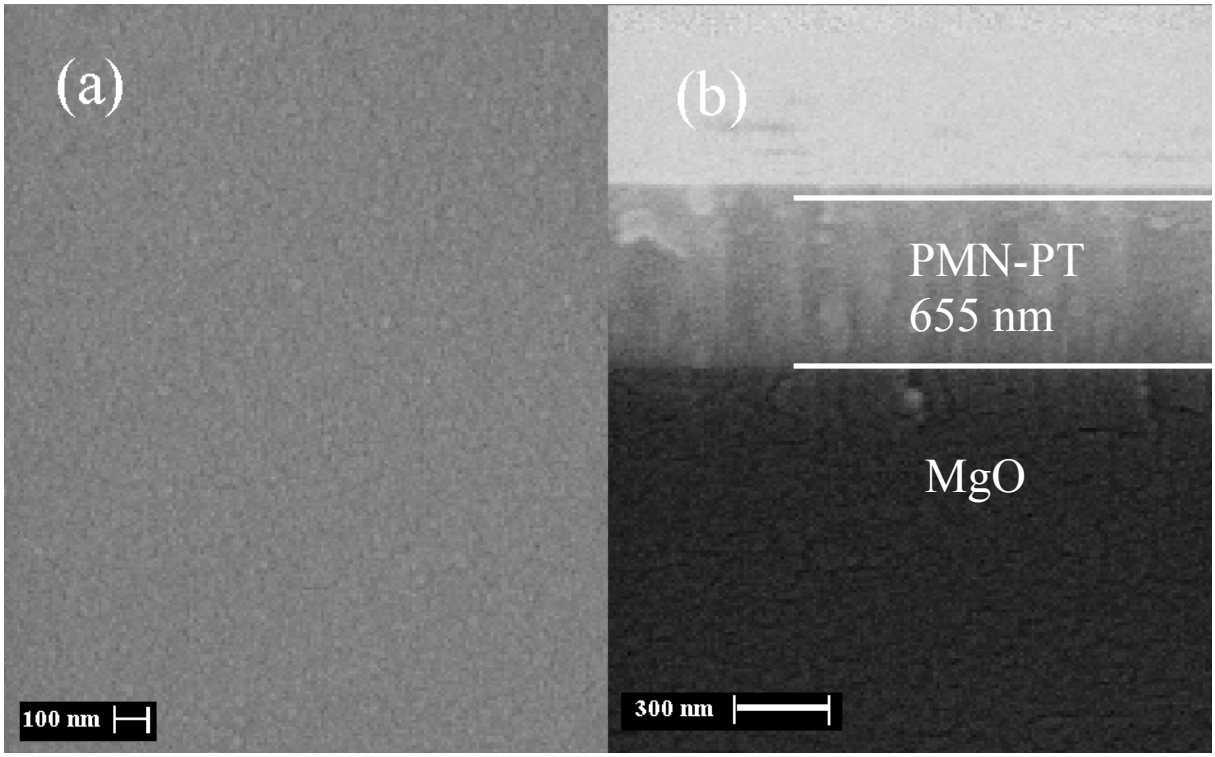

Fig. 2

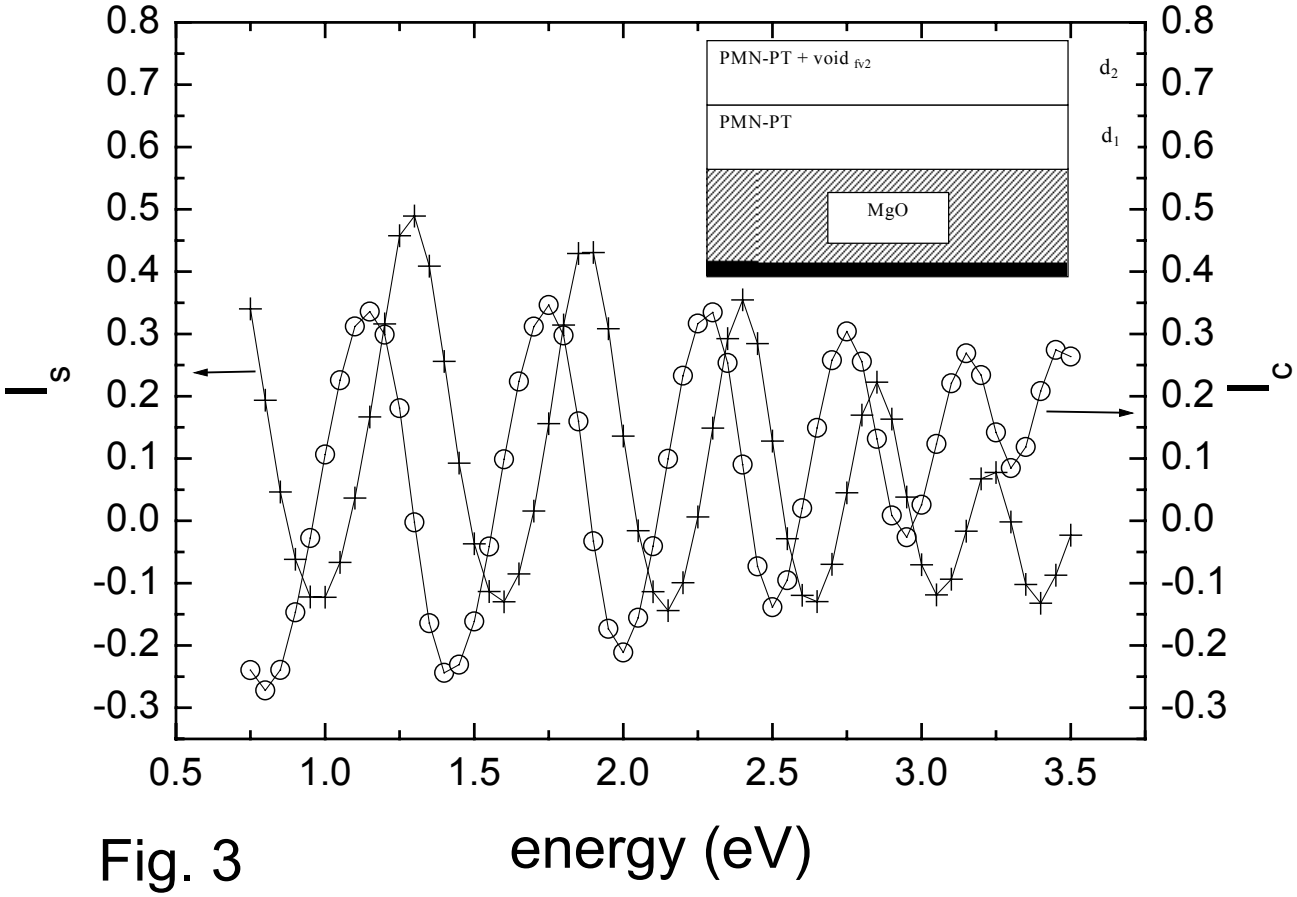
PMN-PT + void fv2
d2
PMN-PT
d1
MgO
Is
Ic
0.8
0.7
0.6
0.5
0.4
0.3
0.2
0.1
0.0
-0.1
-0.2
-0.3
0.5
1.0
1.5
2.0
2.5
3.0
3.5
energy (eV)

Fig. 3

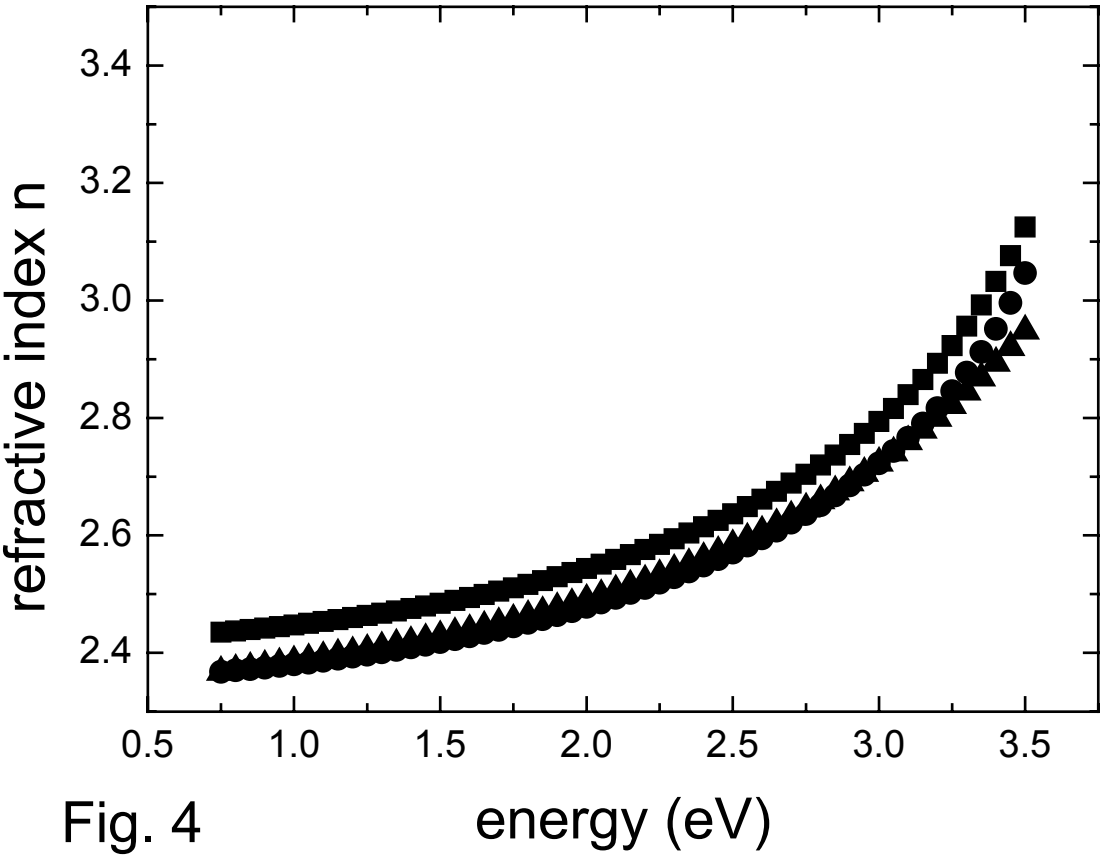
refractive index n
3.4
3.2
3.0
2.8
2.6
2.4
0.5
1.0
1.5
2.0
2.5
3.0
3.5
energy (eV)

Fig. 4

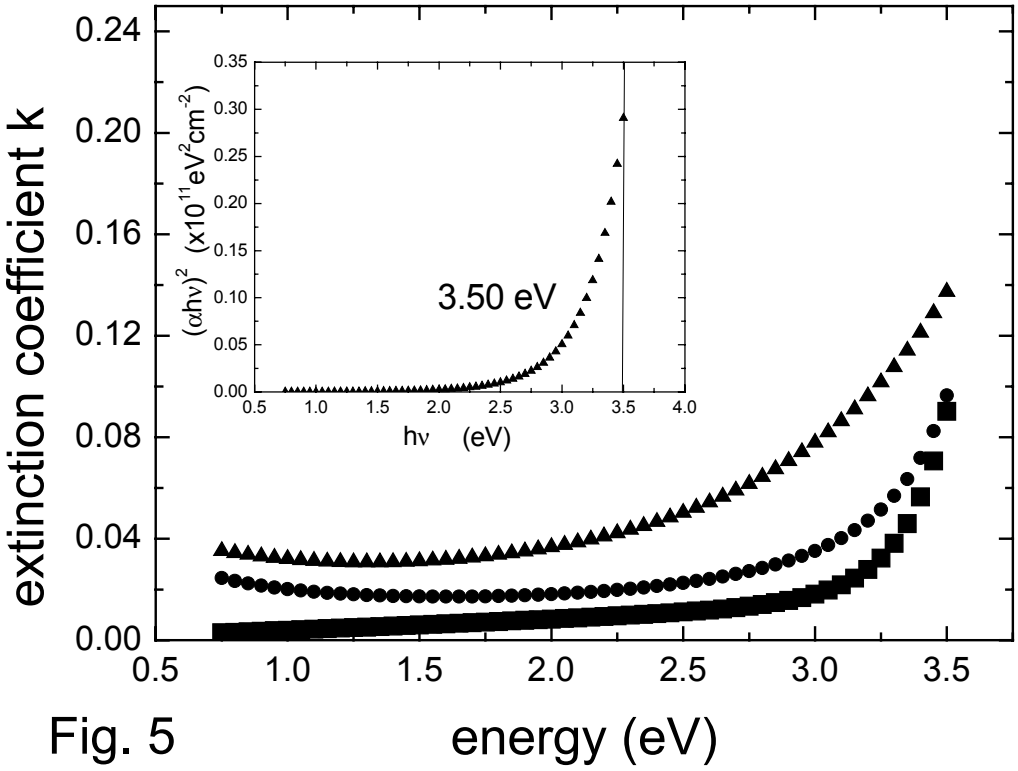
extinction coefficient k
energy (eV)
0.24
0.20
0.16
0.12
0.08
0.04
0.00
0.5
1.0
1.5
2.0
2.5
3.0
3.5
3.50 eV
(αhν)² (x10¹¹eV²cm⁻²)
hν (eV)
0.35
0.30
0.25
0.20
0.15
0.10
0.05
0.00
0.5
1.0
1.5
2.0
2.5
3.0
3.5
4.0

Fig. 5

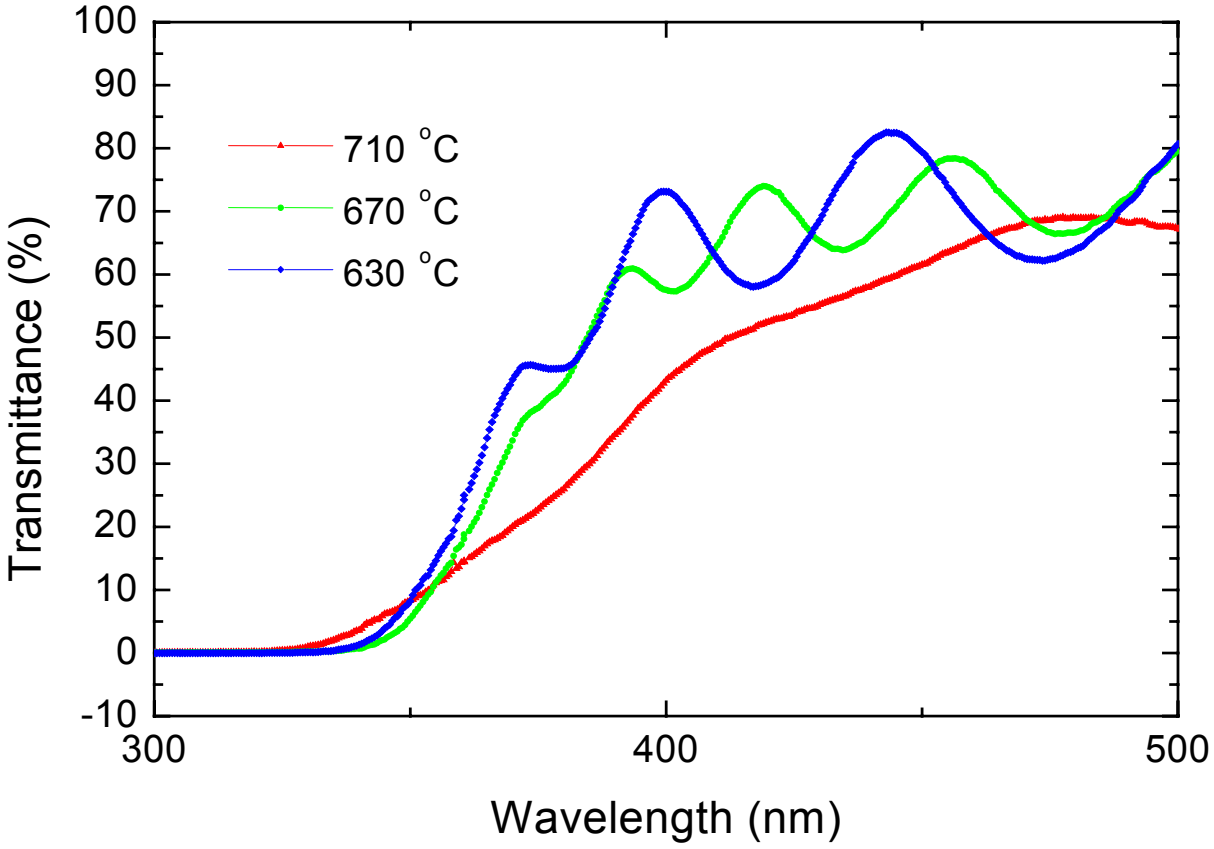
Transmittance (%)
Wavelength (nm)
710 °C
670 °C
630 °C
100
90
80
70
60
50
40
30
20
10
0
-10
300
400
500

Fig. 6

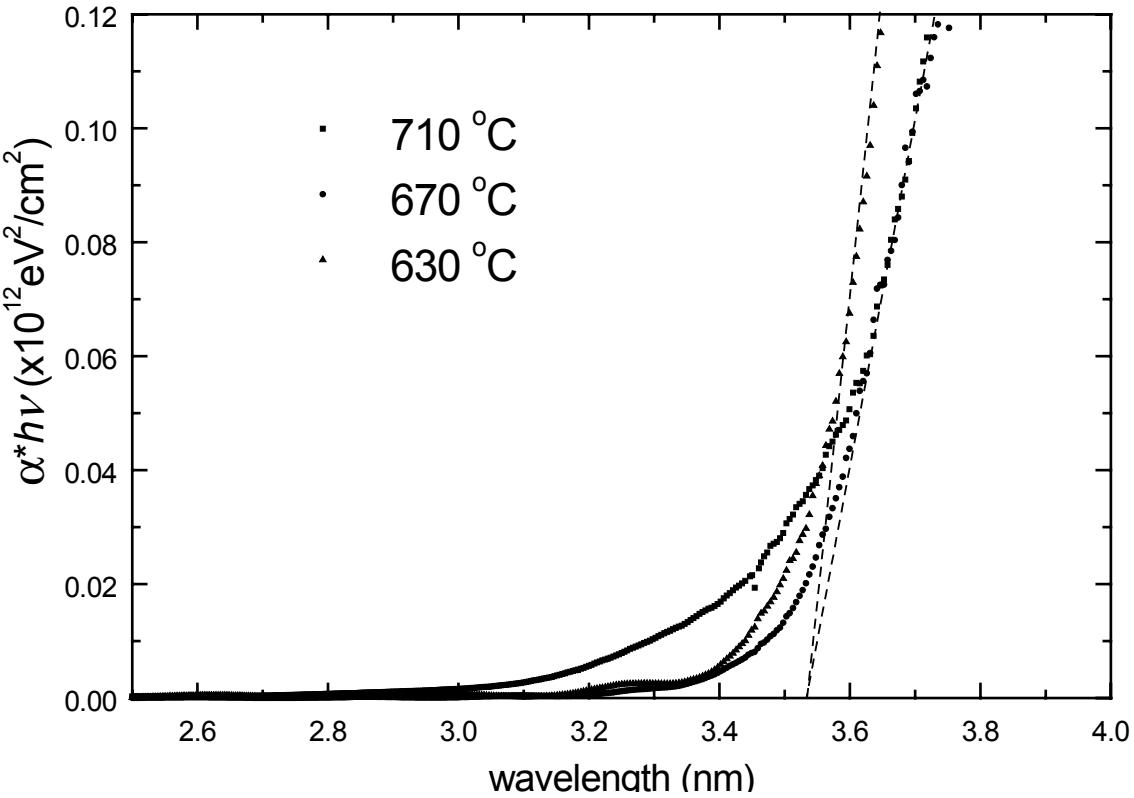
0.12
0.10
0.08
0.06
0.04
0.02
0.00
α*hν (x10^12eV^2/cm^2)
710 °C
670 °C
630 °C
2.6
2.8
3.0
3.2
3.4
3.6
3.8
4.0
wavelength (nm)

Fig. 7

Table I The physical parameters for different PMN-PT films obtained by SE, SEM and AFM.

Deposition temperature / ^{o}C	d_1 (nm)	d_2 (nm)	SEM $d = d_1 + d_2$ (nm)	AFM d_2 (nm)
630	536	2.5	470	4.3
670	538	3.2	655	3.8
710	437	6.6	436	5.5